THE JOURNAL OF PHYSICAL CHEMISTRY Letters

pubs.acs.org/JPCL

Vertically Stacked Molecular Junctions: Toward a Three-Dimensional Multifunctional Molecular Circuit

Elad D. Mentovich,[†,‡] Itsik Kalifa,[‡] Natalie Shraga,[†] Grergory Avrushchenko,[‡] Michael Gozin,[†] and Shachar Richter*[,†,‡]

[†]School of Chemistry, University, Tel Aviv University, Ramat Aviv, Tel Aviv 69978, Israel, and [‡]University Center for Nanoscience and Nanotechnology, Tel Aviv University, Ramat Aviv, Tel Aviv 69978, Israel

ABSTRACT We demonstrate a new method for the construction of three-dimensional vertically stacked molecular junctions. Our approach involves the sequential formation of encapsulated metal−self-assembled monolayer−metal junctions in a three-dimensional configuration, thus forming a molecular circuit. The molecular circuit is constructed at low temperature while utilizing novel process methods in order to minimize possible damage to the molecular layers. We demonstrate this concept by introducing redox-based molecules and proteins into a two-floor molecular circuit and evaluating their electronic properties separately.We show that the electronic molecular "fingerprints" were preserved during the process, and it could be successfully adopted for different types of molecular systems.

SECTION Electron Transport, Optical and Electronic Devices, Hard Matter

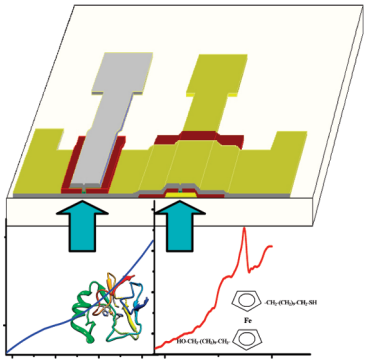

The construction and integration of three-dimensional (3D) electronic devices and circuits have been intensively studied in recent years.[1] This type of architecture offers significant improvement in the efficiency, density, and speed of many types of electronic devices, such as memory arrays and transistors, compared to current very large-scale integration (VLSI) technology.[2] This type of architecture has also been proposed as an alternative solution for increasing computer efficiency without having to dramatically miniaturize the critical size of the device.[3,4]

This impressive technological advance, demonstrated in conventional silicon circuits, has been recently adopted in plastic electronics by the use of nanowires and a soft-lithography technique for the construction of a 3D nanometer-sized circuit. Javey et al.[5] constructed a multilayer nanowire-based structure with layers separated by an insulating material. In their methodology, each layer (floor) was completely isolated from adjacent floors, with no common terminal bridging the floors. Thus, the wiring of such a circuit requires the undesirable assembly of a large number of additional interconnection lines for the activation of simple logic operations.

While the latter example represents a circuit composed of inorganic or polycrystalline materials, adaptation of the 3D configuration to construct circuitry comprising ordered molecules has not yet been demonstrated. As several pioneering papers have shown the feasibility of vertical and planar single-molecule junctions, the integration of several junctions has been only theoretically suggested[6]

Here we demonstrate, for the first time, the construction of 3D architecture using molecular layers as the active building blocks of a molecular circuit. In contrast to previous reports in which each layer was isolated from its neighbors, we suggest a new approach that allows the use of a common electrode for more than one molecular layer, thus paving the way for the future operation of complex molecular computing operations (Figure 1). Since this circuitry requires only a few interconnecting lines for the operation of a large number of active devices per single activation operation, it is also expected to involve minimal power consumption.

Another advantage of our 3D molecular circuits is the possibility of using different types of molecules for each layer, thus increasing its operational versatility. Stan et al. commented on the theoretical potential of such systems and suggested the use of this kind of architecture for various novel computational operations and memory devices that make use of the unique electronic properties of a molecular layer.[6,19]

We have recently shown that a self-assembled monolayer (SAM) comprising special types of electroactive organic molecules can be integrated in a vertical fashion to construct memory devices.[7,8] We further demonstrated the use of such a SAM-based device, containing a redox-based ferrocene (Fc) compound (Figure 1, compound **1**), that utilizes negative-differential-resistance (NDR) behavior.[8] This NDR property was found for other Fc derivatives as well by electrical measurements performed by scanning tunneling microscopy (STM) and conducting atomic-force microscopy (CAFM).[9]

Here we use one of the Fc derivatives as the active component of the bottom-floor device of our 3D molecular circuit.

For the second floor we use a different type of SAM composed of azurin (Az) proteins assembled in a vertical fashion (Figure 1) and utilize it to resolve its unprecedented

Received Date: March 21, 2010
Accepted Date: April 26, 2010
Published on Web Date: April 29, 2010

© 2010 American Chemical Society

DOI: 10.1021/jz100373y | *J. Phys. Chem. Lett.* **2010**, *1*, 1574–1579

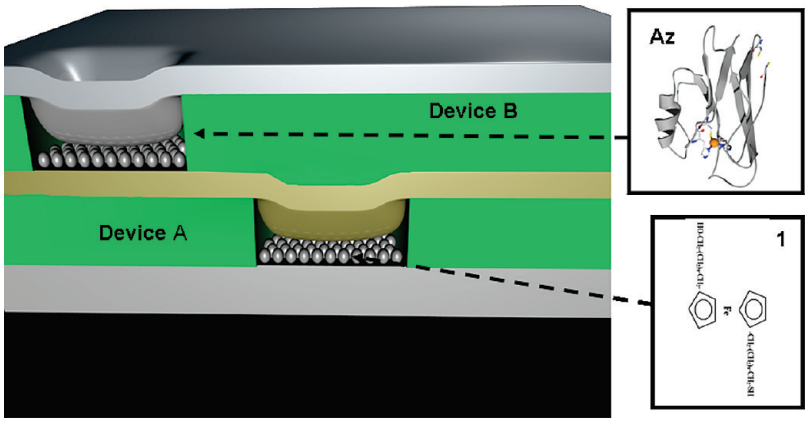

Figure 1. Scheme of the 3D molecular circuit and molecules used. Two molecular devices are connected in vertical fashion (device A, compound **1**; device B, Az). Each individual device is composed of encapsulated SAMs sandwiched between two electrodes.

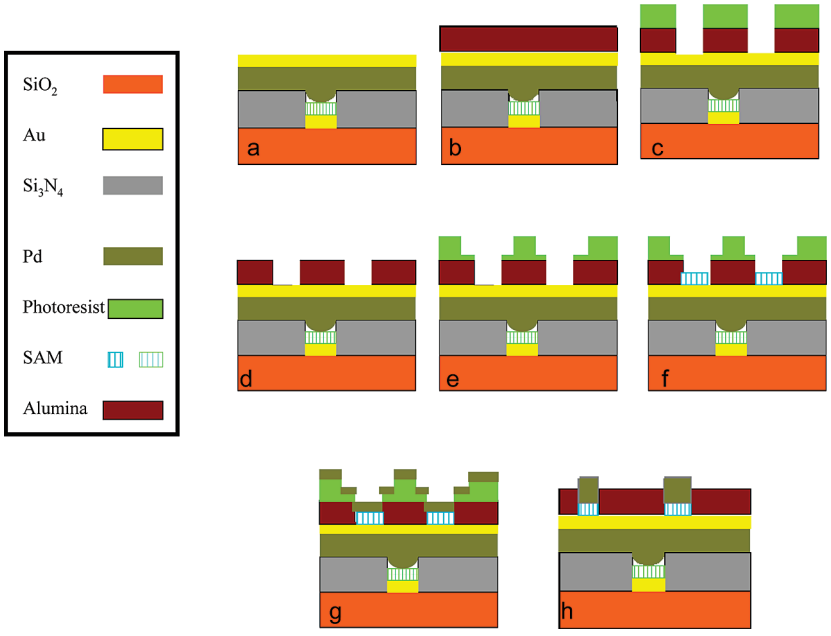

Figure 2. Fabrication process (see Supporting Information for details).

electron transfer (ET) properties in a solid state device configuration.

In recent years, proteins containing redox centers, such as Az, hemoglobin, and photoactive membrane proteins[10] have attracted a great deal of attention due to their unique ET properties in solution[11] and in SAM films.[12] These proteins have been shown to be important in some biological processes, such as photosynthesis, catalysis, and energy-conversion systems.[13]

Basically, there are two known types of ET processes in an assembly of proteins in a solid phase: intramolecular ET, which takes place inside the protein, and intermolecular ET, which takes place between at least two proteins.[14] Rinaldi et al.[15] investigated the intermolecular ET mechanism of an Az-based SAM planar transistor in which the current flows in a direction perpendicular to the SAM, and not through the proteins. Carrier transport through such a device could be explained in terms of the equilibrium between the two possible oxidation states, Cu(I) and Cu(II), existing in the protein. The intermolecular ET mechanism through Az was investigated by Davis et al. with the use of CAFM.[16] This ET was found to be strongly affected by the nature of the Az−AFM contact, which could be mechanically controlled by the AFM tip. When this coupling was weak, an NDR peak was observed, as expected from previous measurements and theory,[17] while stronger coupling resulted in the disappearance of this peak.[18]

The architecture of our device offers a considerable advantage over methods involving scanning-probe microscopy. Whereas in AFM measurements, many experiments are required to gain sufficient statistical data, in our solid-state vertical configuration, one can obtain multiple arrays of stable junctions that can be repeatedly measured and analyzed and also potentially integrated into a molecular circuit.

© 2010 American Chemical Society

DOI: 10.1021/jz100373y | J. Phys. Chem. Lett. 2010, 1, 1574–1579

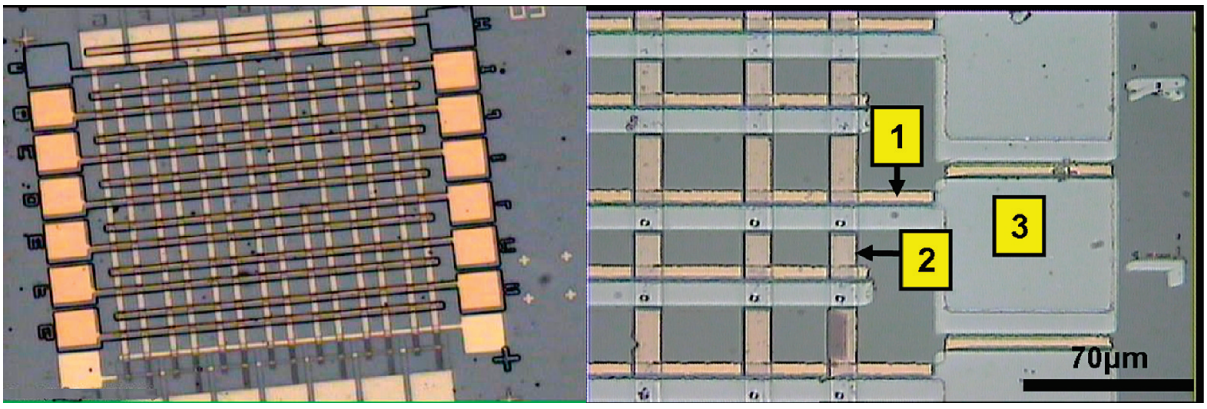

Figure 3. Optical images of the 3D molecular circuit at various stages of the fabrication process. Left: A two-floor 3D molecular circuit after stage f (Figure 2) of the process. Each floor consists of 8 × 8 single devices. Right: The complete 3D molecular circuit featuring the bottom Au (1), middle Au−Pd (2), and top Pd (3) terminals (see Figure 2h for side view scheme).

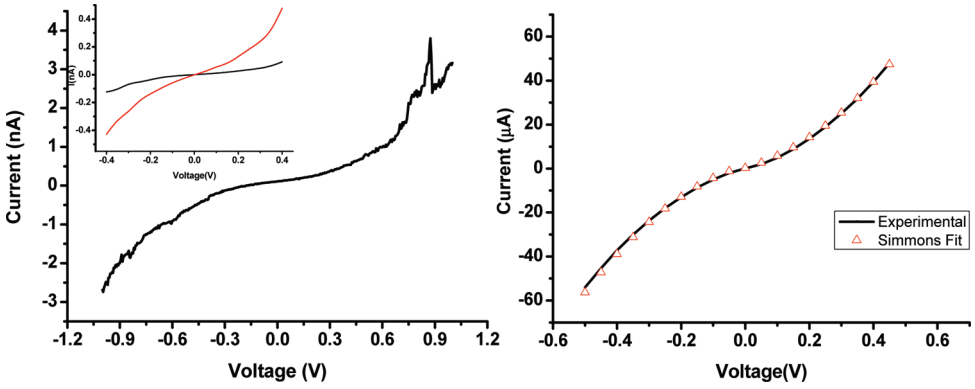

Figure 4. I/V curve taken for the first (left) and second (right) floors. Left: I/V taken for compound **1**. A typical NDR peak is measured. Inset: I/V curve of compound **1** taken before (black) and after (red) the assembly of the second floor. Right: I/V curve (solid line) and Simmons fit (triangles) taken for the Az-SAM located at the second floor. Device's dimensions are approximately 0.02 and 4 μm^2 for the bottom and top floors, respectively.

The photolithography-based fabrication process and optical images of a complete two-floor molecular circuit are shown in Figures 2 and 3 (see Supporting Information for details).

The first floor was constructed with compound **1** serving as the active component with the use of a previously published procedure.[7,8] The same methodology, with minor adjustments to the process flow, was then repeated in order to construct the second floor ,which was composed of the Az-SAM. Here, alumina (Al_2O_3) served as a the dielectric layer (Figure 2b) instead of the silicon nitride used for the first-floor construction. Alumina was chosen because it can be evaporated at low power, providing a high-dielectric material that is also transparent. The transparency of this dielectric layer is highly desirable in that it simplifies the alignment of the different floors. These adjustments were needed in order to reduce possible damage to the bottom floor due to the excessive heating that can be generated in conventional high temperature photolithography processes.[19] Furthermore, one can not duplicate the first-floor process since it involves some high temperature steps (such as e-beam lithography processes and plasma enhanced chemical vapor deposition). Note that the 3D construction process could only be applied because each floor was built on top of a fully aligned and encapsulated SAM in the bottom layer. In principal, this process is not limited to two floors and can be utilized for the construction of an unlimited numbers of floors.

Figure 4 (left) shows a room-temperature current versus voltage (I/V) transport data taken for compound **1** encapsulated in the bottom floor. A clear asymmetrical I/V curve with a distinct imprint of an NDR peak is measured. We and others previously observed this peak.[8] It was attributed either to resonance processes occurring in the metal−SAM−metal junctions or to the two-electron process taking place at the Fc moiety.

We note that the voltage of the NDR peak measured here fits well with previous reports. Several theoretical and experimental studies found redox-center peaks for alkyl-Fc-based molecules near 0.9 V with voltage shifts attributed to either the length of the alkyl chains or to the nature of the metal contacts. Another explanation for this peak could be the existence of a one-step coherent transport process (resonance mechanism) in which an electron tunnels into the redox center (or other empty molecular levels) and to the other metal electrode without relaxation.

© 2010 American Chemical Society

DOI: 10.1021/jz100373y | J. Phys. Chem. Lett. 2010, 1, 1574–1579

However, differences were found between the data obtained for a one-floor device and the current data: first, the aspect ratio of the NDR peak taken in the 3D circuits was found to be much lower than that of a single-floor device, and second, an additional NDR peak at around 0.5 V that is frequently found in Fc-based devices, was not observed here.

Comparison of the two fabrication processes suggests that the thermal treatment performed during the second floor's fabrication process altered the electrical properties of the 3D device. A clear demonstration of this phenomenon can be seen in Figure 4, left (inset), which shows the I/V curves around the origin taken for the first floor before (black) and after (red) the construction of the second floor. It is clearly seen that the thermal treatment increased the current measured in the bottom floor. A similar reduction in the performance of devices stacked in the bottom floor of 3D circuits was recently noted by Seo et al.[20] in the case of plastic transistor devices. They attributed this phenomenon to the longer time of exposure and the larger number of process steps experienced by the first-floor devices during fabrication of the circuit.

In our case, we attribute this change to a possible Pd top-contact modification resulting from the thermal treatment. We have previously indicated that the top contact in a vertical molecular device is extremely process-sensitive, and this can cause considerable change in the location of the NDR peak and its aspect ratio.[8] Since the peak location has not changed and the overall current is on the same order of magnitude, we can eliminate the possibility of filament formation (FF).[21] The latter process would have been expected to show an exponential amplification of the current; this was not observed in our case. Alternatively, a Pd thermal rearrangement without FF can add some additional conduction routes to the molecular junction without causing a dramatic increment in the current . We thus conclude that the Pd-induced thermal damage due to the construction process of the second floor might have reduced the efficiency of the bottom-floor devices.[22]

Figure 4right shows I/V curves of the Az-SAM taken independently in the second floor. In this floor, the cavity diameters were 1 order of magnitude larger than those in the first floor (1−3 μm and 150 nm, respectively). The percentage of working devices decreased dramatically in the large cavities of the second floor (3 μm) compared to the 1 μm cavities, probably as a result of the high concentration of pinholes in the Az-based monolayer that resulted in the shortening of the devices.[23]

Surprisingly, the pattern of the Az I/V curves were almost identical to those obtained by CAFM.[24] The observation that the magnitude of the current measured in our device is much larger than that measured in the scanning probe microscopy (SPM) experiment implies that total current is the result of the ET through a large number of noninteracting Az molecules.

ET analysis of the Az layer was performed with the use of the well-known Simmons-type tunneling model, which assumes charge transport between two electrodes separated by a thin insulating layer.[25]

Here we assume that the barrier height, φ, is higher than the applied voltage, V; hence a modified Simmons formula for the intermediate voltage range can be applied.[25] In this model the current density, J, can be estimated as[24]

$$J = \frac{e}{2\pi h(\beta s)^2}\left\{\left(\varphi - \frac{eV}{2}\right)\exp\left[-\frac{4\pi\beta s}{h}(2m)^{0.5}\left(\varphi - \frac{eV}{2}\right)^{0.5}\right] - \left(\varphi + \frac{eV}{2}\right)\exp\left[-\frac{4\pi\beta s}{h}(2m)^{0.5}\left(\varphi + \frac{eV}{2}\right)^{0.5}\right]\right\}$$

where e and m are the charge and mass of the electron, respectively, s is the thickness of the protein layer, β is the Simmons factor, and h is Planck's constant.

The fitting of this model to our data is shown in Figure 4, right (triangles). The value of φ for this system can be extrapolated with the use of the fitting data,[26] and it is found to be 1.5 eV, thus justifying the assumption of an intermediate-range regime. This value is comparable to the 1.05−1.25 eV values found in a CAFM experiment.[24] Since we assume that each molecule acts as "an independent dielectric material", the ET per molecule can then be estimated by dividing the overall current by the total number of Az molecules inside the cavity ($\sim 10^4$), giving value of several nA/molecule. This value is consistent with previous findings, indicating that protein SAMs in solid-state devices obey scaling rules and thus can be used as stable materials in large-scale molecular devices.[27,28]

The last issue to be addressed in such architecture is the electrical coupling between the floors. Figure 5 shows I/V data taken between the upper contact of the top floor (electrode 3, Figure 3, right) and the bottom contact of the first floor while the middle electrode is disconnected. Thus, this "leakage current" can be measured only if at least one of the floors is shortening. This can be due to several processes such as pinholes and FF. It can be seen that the leakage currents measured are substantially smaller than the currents obtained separately for the first and second floors (which corresponds to a current density of several pA/μm^2 that is at least 4 orders of magnitudes lower than the lowest currents obtained for

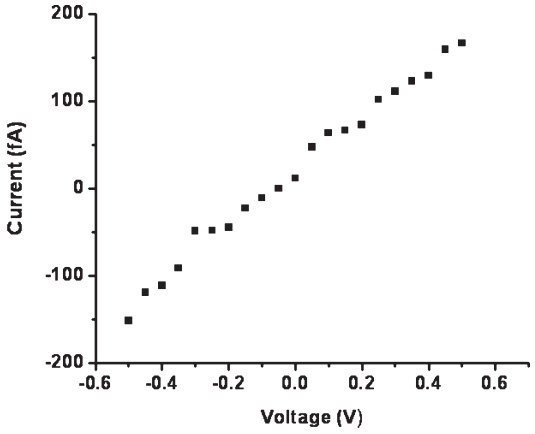

Figure 5. Leakage current measured (in fA) between the top contact of the second floor and the bottom contact of the first floor. The leakage current at high voltages is at least 4 orders of magnitude lower than the lowest currents obtained at similar voltages for individual devices.

© 2010 American Chemical Society

DOI: 10.1021/jz100373y | J. Phys. Chem. Lett. 2010, 1, 1574–1579

similar voltages for individual devices). This observation indicates that the floors are not electrically coupled, and undesired "cross talking" processes do not take place, thus allowing the operation of the vertical circuit.

In conclusion, we have demonstrated a new method for the construction of 3D multifunctional SAM-based vertically stacked molecular junctions. Our approach involves the sequential formation of encapsulated metal−SAM−metal junctions in a 3D configuration to form a molecular circuit.

The electrical properties of each layer can be manipulated by choosing different compounds for each floor. We have demonstrated this concept by introducing redox-based molecules and proteins into a two-floor circuit and evaluating their electronic properties separately.

In the future, this method should allow the assembly of multilayer multifunctional 3D molecular circuits and lead to a new type of dense and fast circuits. In particular, we believe the use of this 3D cross-bar methodology will allow the development of cheap and dense nonvolatile memories crucial for future flash memory technology.

SUPPORTING INFORMATION AVAILABLE Full details of the circuit-fabrication processes and its characterization. SAM spectroscopic FTIR and ellipsometry and I/V measurements of the reference device. This material is available free of charge via the Internet at http://pubs.acs.org.

AUTHOR INFORMATION

Corresponding Author:

*To whom correspondence should be addressed. E-mail: srichter@tau.ac.il.

ACKNOWLEDGMENT The authors thank Mrs. Netta Hendler and Mr. Noam Sidelman for technical support, and Dr. Bogdan Belgorodsky for protein supply. This work was supported by the Clal Biotechnology Fund, USAF (Project No. 073003) and the James Frank Foundation.

REFERENCES

(1) Ahn, J. H.; Kim, H. S.; Lee, K. J.; Jeon, S.; Kang, S. J.; Sun, Y. G.; Nuzzo, R. G.; Rogers, J. A. Heterogeneous Three-Dimensional Electronics by Use of Printed Semiconductor Nanomaterials. *Science* **2006,** *314*, 1754–1757.

(2) Sapatnekar, S.; Nowka, K. Guest Editors' Introduction: New Dimensions in 3D Integration. *IEEE Des. Test Comput.* **2005,** *22*, 496–497.

(3) Rose, G. S.; Yao, Y.; Tour, J. M.; Cabe, A. C.; Gergel-Hackett, N. Majumdar, N.; Bean, J. C.; Harriott, L. R.; Stan, M. R. Designing CMOS/Molecular Memories while Considering Device Parameter Variations. *ACM J. Emerging Technol.* **2007,** *3*, 3–27.

(4) Rose, G. S.; Ziegler, M. M.; Stan, M. R. Large-Signal Two-Terminal Device Model for Nanoelectronic Circuit Analysis. *IEEE Trans. Very Large Scale Integr.* (*VLSI*) *Syst.* **2004,** *12*, 1201–1208.

(5) Javey, A.; Nam, S.; Friedman, R. S.; Yan, H.; Lieber, C. M. Layer-by-Layer Assembly of Nanowires for Three-Dimensional, Multifunctional Electronics. *Nano Lett.* **2007,** *7*, 773–777.

(6) Stan, M. R.; Franzon, P. D.; Goldstein, S. C.; Lach, J. C.; Ziegler, M. M. Molecular Electronics: From Devices and Interconnect to Circuits and Architecture. *Proc. IEEE* **2003,** *91*, 1940–1957.

(7) Meshulam, G.; Rosenberg, N.; Caster, A.; Burstein, L.; Gozin, M.; Richter, S. Construction of Dithiol-Based Nanostructures by a Layer-Exchange Process. *Small* **2005,** *1*, 848–851.

(8) Mentovich, E. D.; Kalifa, I.; Tsukernik, A.; Caster, A.; Rosenberg-Shraga, N.; Marom, H.; Gozin, M.; Richter, S. Multipeak Negative-Differential-Resistance Molecular Device. *Small* **2008,** *4*, 55–58.

(9) Xiao, X. Y.; Brune, D.; He, J.; Lindsay, S.; Gorman, C. B.; Tao, N. J. Redox-Gated Electron Transport in Electrically Wired Ferrocene Molecules. *Chem. Phys.* **2006,** *326*, 138–143.

(10) Frolov, L.; Rosenwaks, Y.; Richter, S.; Carmeli, C.; Carmeli, I. Photoelectric Junctions between GaAs and Photosynthetic Reaction Center Protein. *J. Phys. Chem. C* **2008,** *112*, 13426–13430.

(11) Farver, O.; Canters, G. W.; van Amsterdam, I.; Pecht, I. Intramolecular Electron Transfer in a Covalently Linked Mutated Azurin Dimer. *J. Phys. Chem. A* **2003,** *107*, 6757–6760.

(12) Eley, D. D.; Spivey, D. I. Semiconductivity in Hydrated Hemoglobin. *Nature* **1960,** *188*, 725–725.

(13) Willner, I.; Katz, E. Integration of Layered Redox Proteins and Conductive Supports for Bioelectronic Applications. *Angew. Chem., Int. Ed.* **2000,** *39*, 1180–1218.

(14) Gradinaru, C.; Crane, B. R. Comparison of Intra- vs Intermolecular Long-Range Electron Transfer in Crystals of Ruthenium-Modified Azurin. *J. Phys. Chem. B* **2006,** *110*, 20073–20076.

(15) Maruccio, G.; Biasco, A.; Visconti, P.; Bramanti, A.; Pompa, P. P.; Calabi, F.; Cingolani, R.; Rinaldi, R.; Corni, S.; Di Felice, R.; et al. Towards Protein Field-Effect Transistors: Report and Model of Prototype. *Adv. Mater.* **2005,** *17*, 816–822.

(16) Davis, J. J.; Wang, N.; Morgan, A.; Zhang, T. T.; Zhao, J. W. Metalloprotein Tunnel Junctions: Compressional Modulation of Barrier Height and Transport Mechanism. *Faraday Discuss.* **2006,** *131*, 167–179.

(17) Xue, Y. Q.; Datta, S.; Hong, S.; Reifenberger, R.; Henderson, J. I.; Kubiak, C. P. Negative Differential Resistance in the Scanning-Tunneling Spectroscopy of Organic Molecules. *Phys. Rev. B* **1999,** *59*, R7852–R7855.

(18) Axford, D.; Davis, J. J.; Wang, N.; Wang, D. X.; Zhang, T. T.; Zhao, J. W.; Peters, B. Molecularly Resolved Protein Electromechanical Properties. *J. Phys. Chem. B* **2007,** *111*, 9062–9068.

(19) Seunarine, K.; Meredith, D. O.; Riehle, M. O.; Wilkinson, C. D. W.; Gadegaard, N. Biodegradable Polymer Tubes with Litho Graphically Controlled 3D Micro- and Nanotopography. *Microelectron. Eng.* **2008,** *85*, 1350–1354.

(20) Seo, S. M.; Baek, C.; Lee, H. H. Stacking of Organic Thin Film Transistors: Vertical Integration. *Adv. Mater.* **2008,** *20*, 1994–1997.

(21) Waser, R.; Aono, M. Nanoionics-Based Resistive Switching Memories. *Nat. Mater.* **2007,** *6*, 833–840.

(22) Mccarley, R. L.; Dunaway, D. J.; Willicut, R. J. Mobility of the Alkanethiol Gold(111) Interface Studied by Scanning Probe Microscopy. *Langmuir* **1993,** *9*, 2775–2777.

(23) Haick, H.; Cahen, D. Making Contact: Connecting Molecules Electrically to the Macroscopic World. *Prog. Surf. Sci.* **2008,** *83*, 217–261.

(24) Zhao, J. W.; Davis, J. J.; Sansom, M. S. P.; Hung, A. Exploring the Electronic and Mechanical Properties of Protein Using Conducting Atomic Force Microscopy. *J. Am. Chem. Soc.* **2004,** *126*, 5601–5609.

© 2010 American Chemical Society

(25) Simmons, J. G. Generalized Formula for the Electric Tunnel Effect between Similar Electrodes Separated by a Thin Insulating Film. *J. Appl. Phys.* **1963,** *34*, 1793–1803.
(26) Vilan, A. Analyzing Molecular Current−Voltage Characteristics with the Simmons Tunneling Model: Scaling and Linearization. *J. Phys. Chem. C* **2007,** *111*, 4431–4444.
(27) Green, J. E.; Choi, J. W.; Boukai, A.; Bunimovich, Y.; Johnston-Halperin, E.; DeIonno, E.; Luo, Y.; Sheriff, B. A.; Xu, K.; Shin, Y. S. A 160-Kilobit Molecular Electronic Memory Patterned at 10(11) Bits Per Square Centimetre. *Nature* **2007,** *445*, 414–417.
(28) Akkerman, H. B.; Blom, P. W. M.; de Leeuw, D. M.; de Boer, B. Towards Molecular Electronics with Large-Area Molecular Junctions. *Nature* **2006,** *441*, 69–72.

© 2010 American Chemical Society

DOI: 10.1021/jz100373y | *J. Phys. Chem. Lett.* **2010,** *1*, 1574–1579